Int. J. Electrochem. Sci., 16 (2021) 150912, doi: 10.20964/2021.01.29

International Journal of
ELECTROCHEMICAL
SCIENCE
www.electrochemsci.org

Corrosion Behavior of ZrCrMoNb High-entropy Alloy Coating in Ethylene Glycol Solution

Hanyang Zuo[1,4] , *Long Wang*[4], *Min Gong*[1,3*], *Xingwen Zheng*[2, 3], *Chunhai Liu*[4], *Jinlong Fan*[1,3], *Feng Liu*[1,3] ,

[1] School of Material and Science Engineering, Sichuan University of Science & Engineering, Zigong 643000, China
[2] School of Chemical and Environmental Engineering, Sichuan University of Science & Engineering, Zigong 643000, China
[3] Key Laboratory of Material Corrosion and Protection of Sichuan Province, Zigong 643000, China
[4] Southwestern Institute of Physics, Chengdu 610225, China
[5] College of Materials and Chemistry & Chemical Engineering, Chengdu University of Technology, Chengdu 610225, China
[*]E-mail: gmsuse@126.com

Received: 4 September 2020 / *Accepted:* 10 November 2020 / *Published:* 30 November 2020

A novel ZrCrMoNb high-entropy alloy coating was prepared on 3A21 aluminum alloy and its corrosion behavior in ethylene glycol solution was studied. By polarization curve, electrochemical impedance spectroscopy (EIS) and scanning electron microscope (SEM), the effects of temperature and concentration of ethylene glycol on corrosion behavior of ZrCrMoNb high-entropy alloy coatings were analyzed. The results show that the corrosion resistance of ZrCrMoNb high-entropy alloy coating degraded with the increase of temperature, and the corrosion current density of ZrCrMoNb high-entropy alloy coating in ethylene glycol solution decreases significantly when the V/V concentration ethylene glycol changes from 15% to 30%, after that, the corrosion current density changed little with the increase of ethylene glycol concentration. Scanning electron microscope results display that the coating can improve the pitting corrosion resistance of 3A21 aluminum alloy in ethylene glycol solution.

Keywords: High-entropy alloy coating; ZrCrMoNb coating; Ethylene glycol solution; corrosion

1. INTRODUCTION

With the advancement of microelectronic technology, military electronic equipment continues to develop toward high power, high density, and high frequency, resulting in a sharp increase in the heat flux density of electronic equipment. At this time, higher requirements are placed on the cooling technology. The cold plate system of military electronic equipment can take away the heat dissipation

of the electronic components installed on it by forced convection heat exchange[1]. Aluminum alloy was widely used in the cold plate system of military electronic equipment because of its good thermal conductivity, low density, good corrosion resistance and easy processing. Ethylene glycol solution as a common coolant, would oxidize and decompose to form organic acids such as glycolic acid and oxalic acid during service, resulting in increased corrosion, thus, which may lead to the destruction of aluminum alloy due to corrosion and further affect the normal operation of the equipment[2].

In the past few decades, both organic and inorganic coatings have been widely used to protect metals from corrosion. Shen [3] found the corrosion resistance of 6061 aluminum alloys could been improved by high-temperature oxidation pre-treated micro-arc oxidation, normal micro-arc oxidation and high-temperature oxidation pretreatment, normal micro-arc oxidation showed the best corrosion resistance. The high-entropy alloy coating uses a random arrangement of multiple elements in the form of a solid solution to create a locally disordered chemical environment. Aluminum alloy had made some research progress in coating. Zhao [4] showed that chromate will form a Cr-enriched film on the surface of Al 2024-T3, increasing the corrosion resistance of Al 2024-T3. Yeh [5] first proposed the concept of high-entropy alloys, about 16 years ago. The high-entropy alloy coating is randomly arranged through a variety of elements in the form of solid solution, creating a locally disordered chemical environment[5]. Because the high-entropy alloy is composed of unique multiple main elements, it has many ideal properties[6]. The high-entropy alloy has excellent characteristics such as excellent high-temperature oxidation resistance, good corrosion resistance, and excellent wear resistance[7-12]. The high-entropy alloy coating can be deposited on the substrate surface by magnetron sputtering technology and magnetron co-sputtering technology[13-15]. Therefore, high-entropy alloys are highly valued in materials science and engineering. However. There are few reports about the effect of high-entropy alloy coatings on the corrosion behavior of aluminum alloys in ethylene glycol solutions.

In this study, a high-entropy alloy coating was used as a protective coating for 3A21 aluminum alloys in ethylene glycol solutions. According to the corrosion environment of aluminum alloys, high-entropy alloy coatings are composed of four elements (Zr, Cr, Mo and Nb). The coating was made on the surface of aluminum alloy by magnetron sputtering technology[13-15]. The corrosion behavior of the coating in ethylene glycol solution was studied by electrochemical method. The effects of ethylene glycol concentration and temperature on the corrosion behavior of the coating in ethylene glycol solution were discussed.

2. EXPERIMENTAL

2.1 Preparation of high entropy alloy coating

The ZrCrMoNb high-entropy alloy coating were deposited on 3A21 aluminum alloy substrates by magnetron sputtering technology. Four types of element metal targets of Zr, Cr, Mo and Nb with a purity 99.99% were used. Prior to each coating co-sputtering experiment, the sample was successively wet ground using silicon carbide abrasive paper with increased fineness until it reached 800 grits, degreased with acetone and absolute ethanol to remove oil, rinsed with distilled water and then air-dried.

The Ar gas flow rate was fixed at 300Sccm, and the working pressure was maintained at 0.4 Pa by controlling the throttle valve. The sputtering power of ZrCrMoNb was 150W, and the sputtering time was 20 minutes, so the thickness of the ZrCrMoNb coating produced was about 3μm.

2.2 Characterization Electrochemical equipment and measurements

Electrochemical measurements were performed a potentiostat (Solartron SI 1287 Electrochemical interface/Solartron SI 1260 Impedance gain-phase analyzer), and controlled by Zplot and Corrware software. A conventional three-electrode system was used in the experiment, ZrCrMoNb high-entropy alloy based on aluminum alloy was used as working electrode, and its working area was 0.785 cm^2, a platinum grid and a saturated calomel electrode (SCE) were used as the counter electrode and the reference electrode, respectively.

The open circuit potential (OCP) was first tested for 30 minutes in order to make the electrode surface in a stable state, then the EIS measurements were carried out at the open circuit potential (OCP) with AC signals of 5 mV amplitude in a frequency range of 100 kHz to 0.01 Hz. The impedance spectra were fitted by ZSimpWin software and Zplot. The potentiodynamic polarization test was conducted at a scan rate of 1 mV/s in the potential range of -0.3 V to +0.3 mV versus OCP.

The corrosion solution was prepared by dissolving 148 mg of anhydrous sodium sulfate, 165 mg of sodium chloride and 138 mg of sodium bicarbonate in 1 L of distilled water according to ASTM D1384-01[16]. Ethylene glycol solution was prepared was with corrosive solution and ethylene glycol according to the volume ratio. The experimental V/V concentrations of ethylene glycol were 15%, 30%, 50%, 65% and 80%, respectively. In this experiment, the temperatures were 25°C, 55°C, and 88°C. The schematic diagram of the experimental device was shown in the Fig. 1.

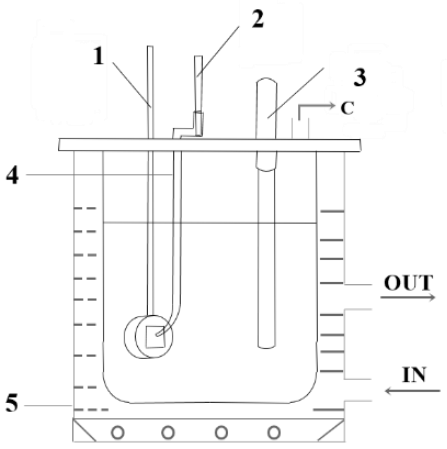

Figure 1. The diagram of the experimental device: 1, working electrode; 2, reference electrode; 3, counter electrode; 4, salt bridge and Luggin capillary; 5, circulating water heating system; C, connected to a condenser.

2.3 Surface analysis

The surface morphology of each sample after electrochemical measurement was observed by scanning electron microscope (SEM, TESCAN Vega-3 SBU) equipped with energy-dispersive X-ray spectroscopy (EDS, BRUKER D2-PHASER).

3. RESULTS AND DISCUSSION

3.1 ZrCrMoNb Coating

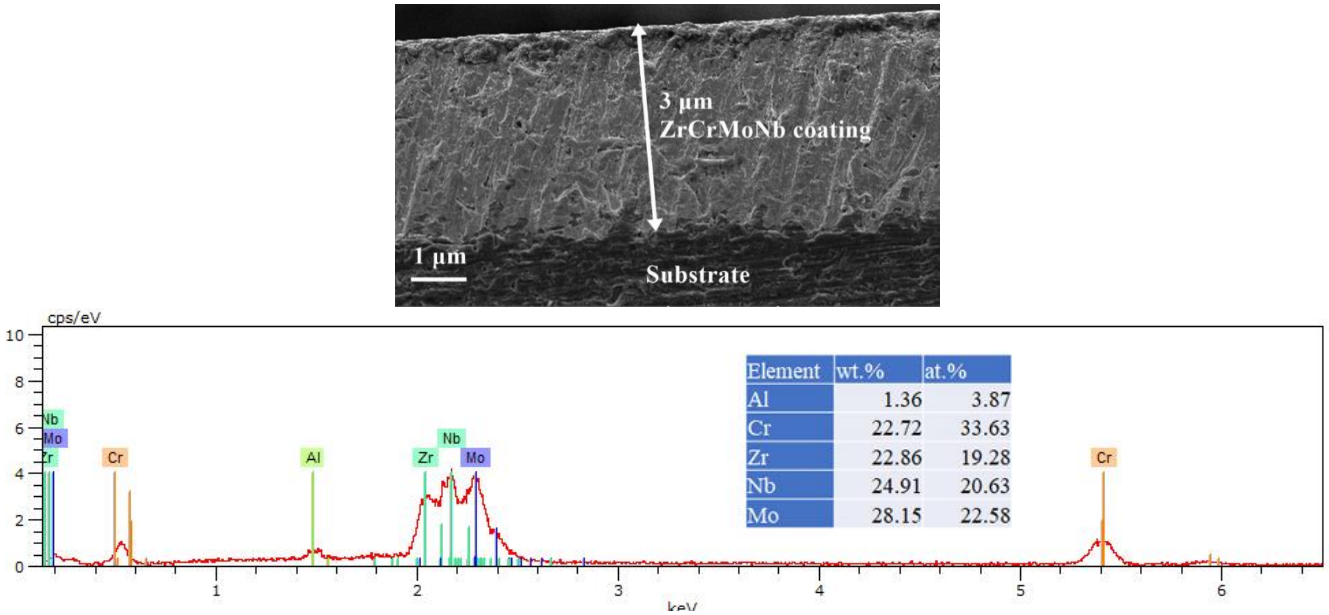

Figure 2. Cross-sectional SEM image and EDS micrographs of the ZrCrMoNb high-entropy alloy coating based on 3A21 aluminum alloy.

Fig. 2 is shown was that a uniform the ZrCrMoNb coating was deposited on the surface of the aluminum alloy, and the thickness of the coating was about 3 μm. The result of EDS shows that the distribution of the four metal elements (Zr, Cr, Mo and Nb) on the surface of the coating was relatively uniform, while there would also be a little aluminum element in the coating, which might be the result of polishing the cross section of the sample.

3.2 Potentiodynamic polarization

As shown in the Fig. 3, in the same concentration of ethylene glycol solution, the corrosion potential (E_{corr}) showed a negative shift trend with increasing temperature, and the amplitude of negative shift increases with the increase of glycol concentration, which can be seen more clearly from Fig. 4. As shown in Fig. 4, at the same temperature, when the V/V concentration of ethylene glycol is between 15% and 50%, the corrosion potential increases slowly with the increase of concentration, but the overall

change was not significant. However, when the V/V concentration of ethylene glycol reaches 65%, the corrosion potential obviously shifts negatively, and then shows different trends with different temperatures. All these may reflect the influence of concentration and temperature on the reaction mechanism of the ZrCrMoNb high-entropy alloy coating in ethylene glycol solution.

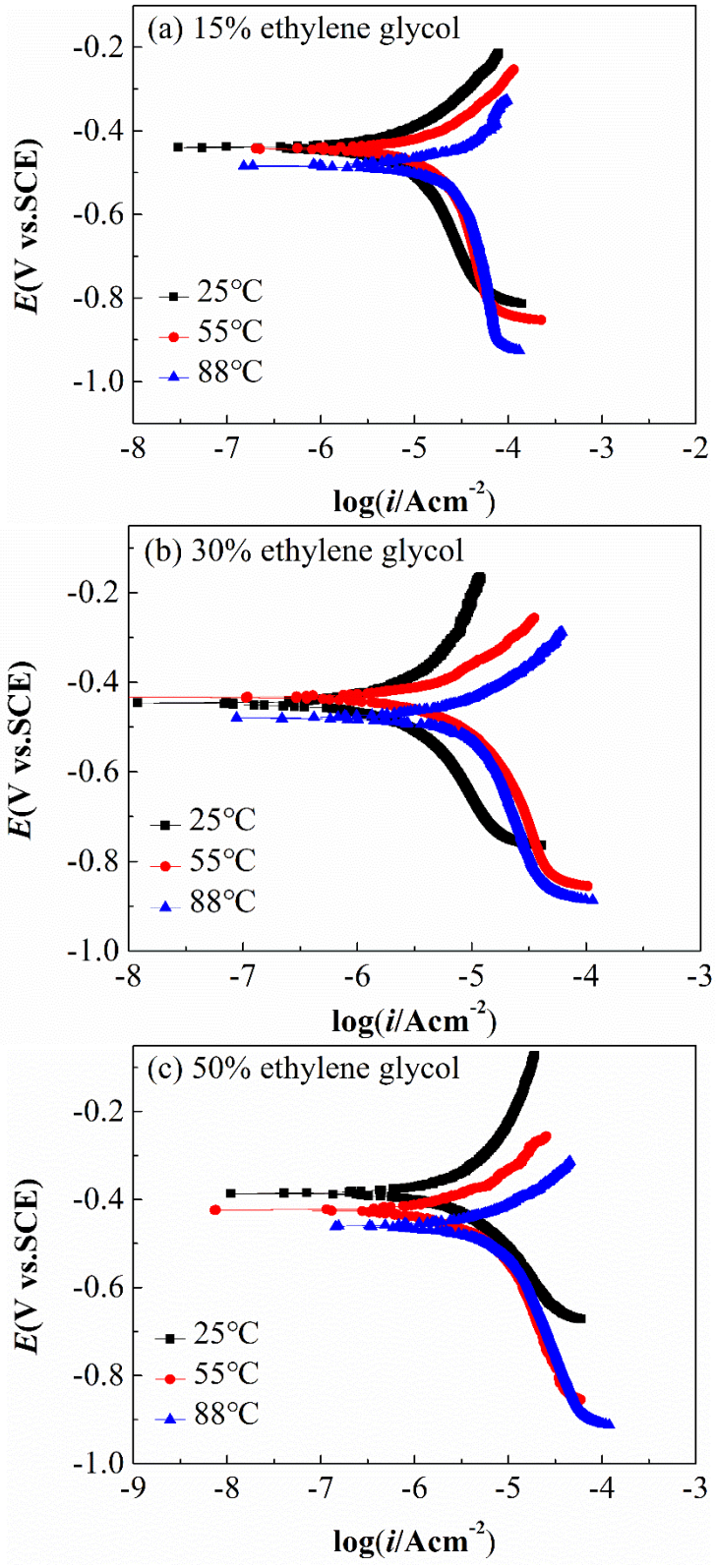

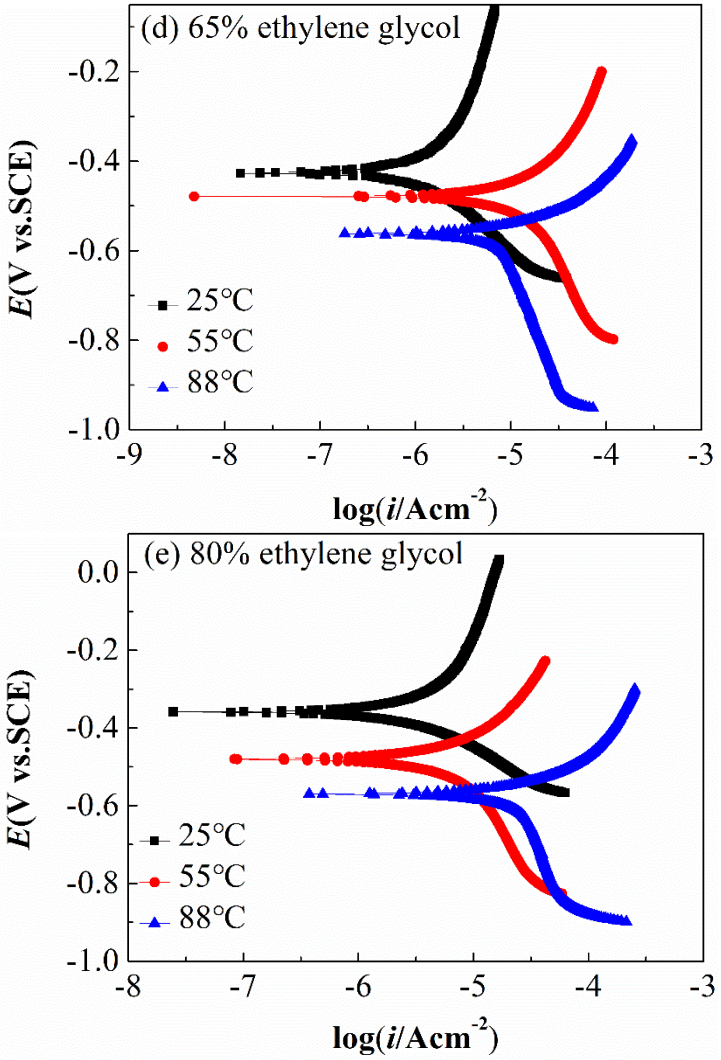

Figure 3. Potentiodynamic polarization curves of the ZrCrMoNb high-entropy alloy coating based on 3A21 aluminum alloy in different concentrations of ethylene glycol solution at different temperatures: (a)15% EG; (b) 30% EG; (c) 50% EG; (d) 65% EG; (e) 80% EG.

It is also seen from Fig. 3 that, in the same concentration of ethylene glycol solution, the corrosion current density (I_{corr}) had a tendency to increase with increasing temperature due to the intensified molecular thermal motion under increased temperature. The corrosion current density of the ZrCrMoNb high-entropy alloy coating based on 3A21 aluminum alloy in different concentrations of ethylene glycol solution at different temperatures is given in Fig. 5. It can be seen that the corrosion current density first decreases and then increases with the increase of glycol concentration, and this trend becomes more obvious with the increase of temperature. Ethylene glycol is a polar molecule, which can be adsorbed on the metal surface, meanwhile, with the increase of ethylene glycol concentration, the viscosity of the solution increases, the migration of ions and the diffusion of oxygen will be inhibited, thus reducing the corrosion rate. However, when the concentration of ethylene glycol solution reaches a certain concentration, the corrosion rate increases, which may reflect the change of reaction mechanism,

especially at high temperature, the effect of the decrease of dissolved oxygen on the reaction mechanism becomes more significant. This is also reflected in the change of corrosion potential.

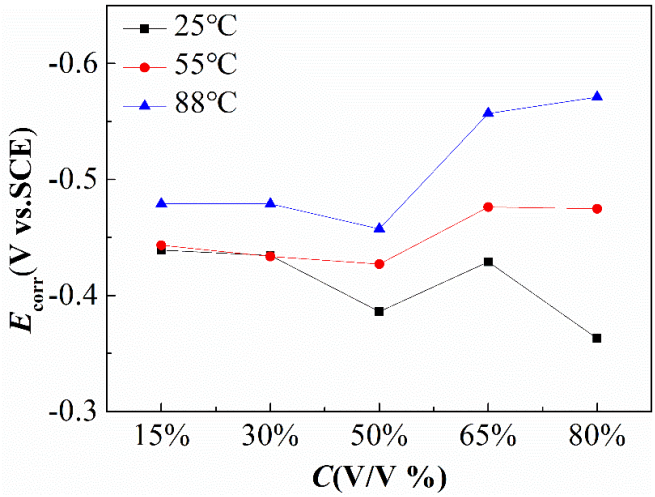

Figure 4. Corrosion potential of the ZrCrMoNb high-entropy alloy coating based on 3A21 aluminum alloy in different concentrations of ethylene glycol solution at different temperatures.

It is also noted that, the corrosion current density decreases significantly when the V/V concentration ethylene glycol changes from 15% to 30%, after that, the corrosion current density changed little with the increase of ethylene glycol concentration, except in 80% ethylene glycol solution at 88 ℃, therefore, 30% V/V concentration of ethylene glycol might be a critical concentration for the corrosion of ZrCrMoNb high-entropy alloy coating based on 3A21 aluminum alloy in ethylene glycol solution.

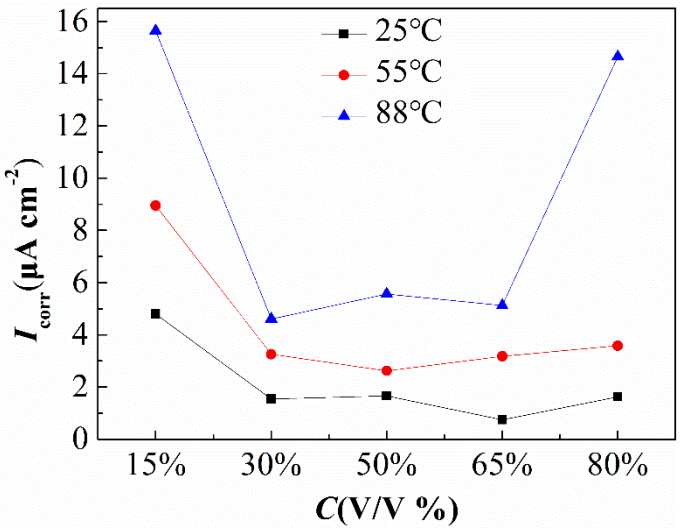

Figure 5. Corrosion current density of the ZrCrMoNb high-entropy alloy coating based on 3A21 aluminum alloy in different concentrations of ethylene glycol solution at different temperatures.

Moreover, according to the research results of Harish[17], the corrosion current of Mg-Al-Zn-Mn alloy reached 10.09 μA/cm^{-2} in 30% V/V concentration ethylene glycol at 30°C, correspondingly, the corrosion current of the ZrCrMoNb coating in 30% V/V concentration ethylene glycol is only 1.54 μA/cm^{-2} at 55°C, indicating that the ZrCrMoNb high-entropy alloy coating has good corrosion resistance.

3.3 Electrochemical Impedance Spectroscopy

Fig. 6 shows the electrochemical impedance spectroscopy (EIS) of ZrCrMoNb high-entropy alloy coating based on 3A21 aluminum alloy in different V/V concentrations of ethylene glycol solution at different temperatures. The impedance spectrum of the coating presents as an incomplete semicircle under most experimental conditions. However, when the V/V concentration of ethylene glycol is 65% and 80% at temperature of 25℃, the Warburg impedance appears in the impedance spectrum, which may be related to the diffusion of corrosion products due to the higher viscosity of ethylene glycol at high concentrations. The appearance of the Warburg impedance involves the corrosion process of oxygen diffusion[18, 19]. Meanwhile, polarization resistance R_p is not a finite value and cannot be determined in this case. Another case is that the temperature is 88 ℃ and the V/V concentration of ethylene glycol is 80%, the impedance spectrum consists of a high-frequency semicircle and a low-frequency semicircle. The impedance spectra show different shapes under different experimental conditions, which reflects the change of reaction mechanism, as shown in the polarization curves.

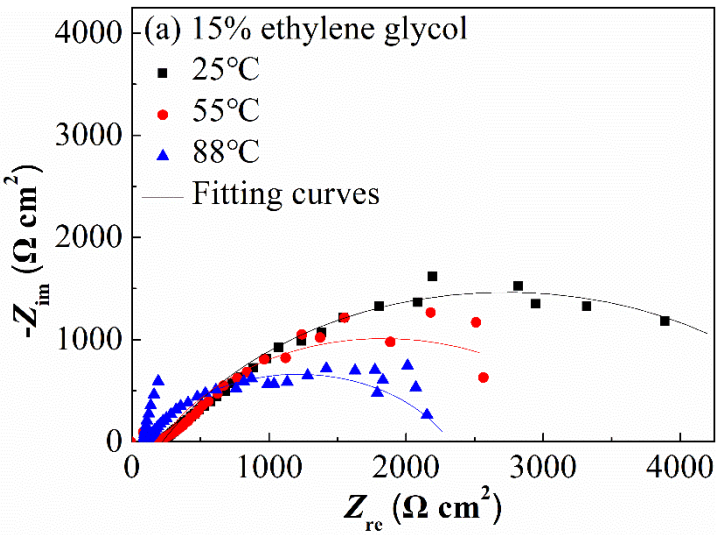

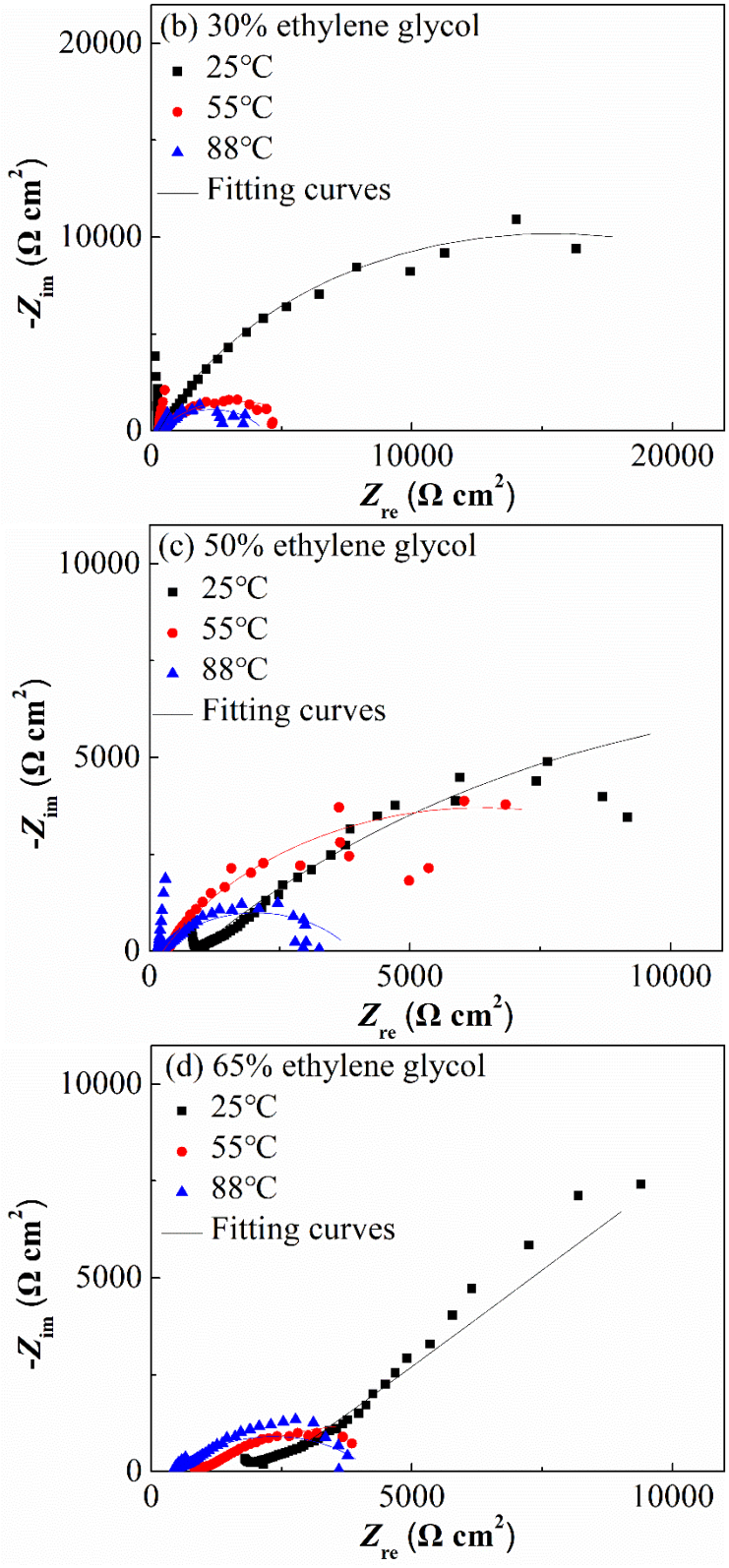
(b) 30% ethylene glycol
25°C
55°C
88°C
Fitting curves
20000
10000
0
0
10000
20000
$-Z_{im}$ (Ω cm^2)
Z_{re} (Ω cm^2)
(c) 50% ethylene glycol
25°C
55°C
88°C
Fitting curves
10000
5000
0
0
5000
10000
$-Z_{im}$ (Ω cm^2)
Z_{re} (Ω cm^2)
(d) 65% ethylene glycol
25°C
55°C
88°C
Fitting curves
10000
5000
0
0
5000
10000
$-Z_{im}$ (Ω cm^2)
Z_{re} (Ω cm^2)

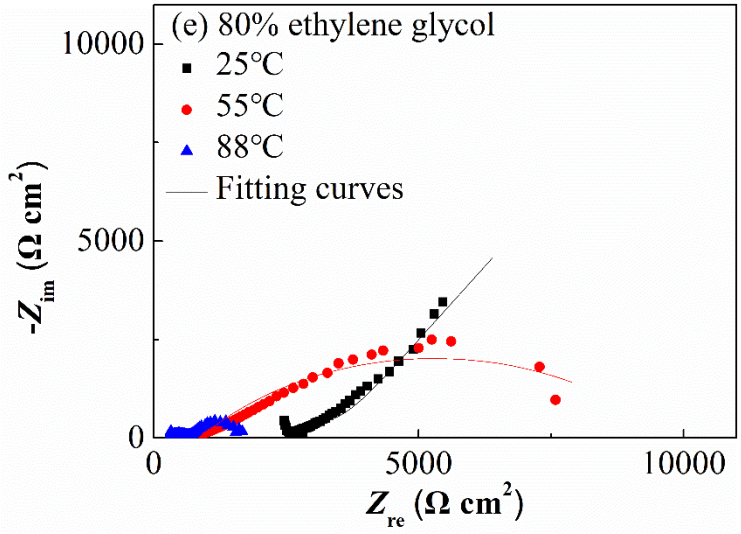

Figure 6. The EIS of the ZrCrMoNb high-entropy alloy coating based on 3A21 aluminum alloy in different concentrations of ethylene glycol solution at different temperatures: (a)15% EG; (b) 30% EG; (c) 50% EG; (d) 65% EG; (e) 80% EG.

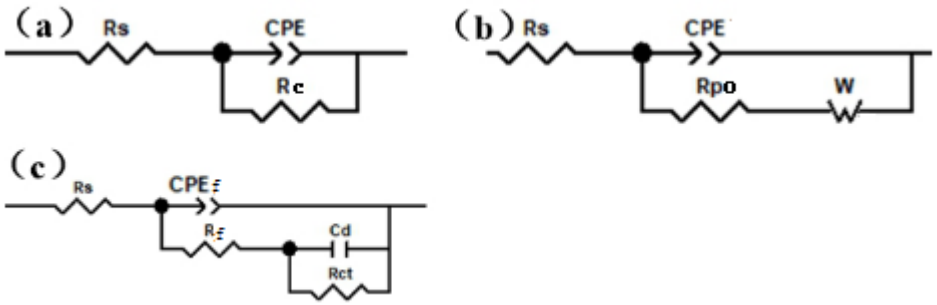

Figure 7. The equivalent circuits used to fit the EIS data.

According to the characteristics of impedance spectrum, three equivalent circuits as shown in Fig. 7 were used to fit the EIS data under different experimental conditions. In the equivalent circuit, R_s is the solution resistance, R_c is the caotaing resistance, R_{po} is the pore resistance, CPE is the coating capacitance, and W is Warburg impedance[16, 20], CPE_f and R_f respectively represent the capacitance and resistance of oxide film, C_d is the electric double layer capacitor, R_{ct} is the charge transfer resistance. To improve the accuracy of the simulation in the case of dispersion effects, a surface inhomogeneity factor and a possible diffusional factor were included, a constant phase angle element (CPE) is often used to replace the ideal capacitance[21]. The capacitive element is represented by the following equation[22, 23].

$$Z_Q = \frac{1}{Y_0(jw)^n} \tag{1}$$

where j is an imaginary unit ($j^2 = -1$) and w is the angular frequency ($w = 2\pi f$).Y_0 denotes a frequency-independent constant; and n ($1 \leq n \leq 1$) is the parameter of CPE[24]. The polarization resistance represents the corrosion resistance of the coating[25, 26], It can be obtained by $R_p = R_c$ in

Fig.7(a) and $R_p = R_f + R_{ct}$ in Fig.7(c), and the fitting result is shown in the Fig. 8. R_p is not a finite value and cannot be determined in Fig. 7(b) due to the Warburg impedance, the pore resistance R_{po} is given in Fig. 8.

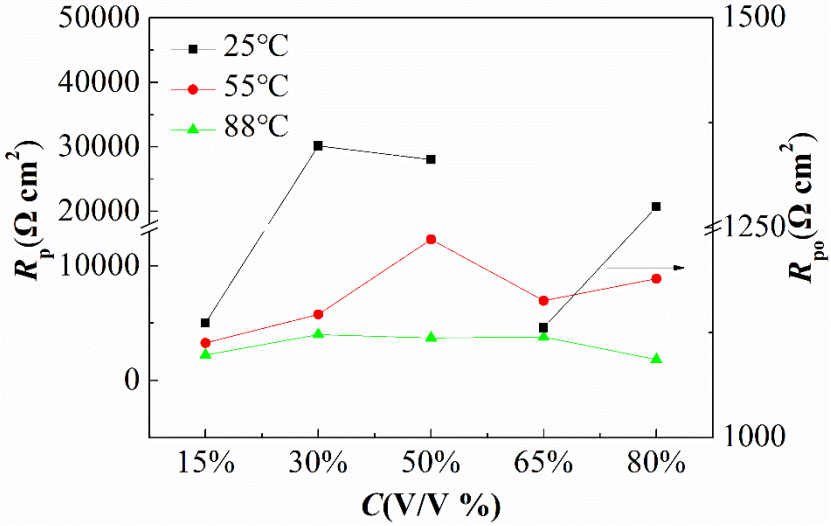

Figure 8. R_p of the ZrCrMoNb high-entropy alloy coating based on 3A21 aluminum alloy in different concentrations of ethylene glycol solution at different temperatures.

As shown in the Fig. 8, in the same concentration of ethylene glycol solution, the values of R_p decrease with rising temperature, which indicates that the corrosion rate increases with the increase of temperature, which is consistent with the results of polarization curve. However, under the same temperature, with the increase of ethylene glycol concentration, the values of R_p first increase and then decrease, the trend is opposite to that of corrosion current density, and the possible reason has been described before. At a temperature of 25°C, when the V/V concentration of ethylene glycol changes from 65% to 80%, the pore resistance R_{po} increases, this may correspond to the diffusion of ions in the pores of the coating.

3.4 Surface analysis

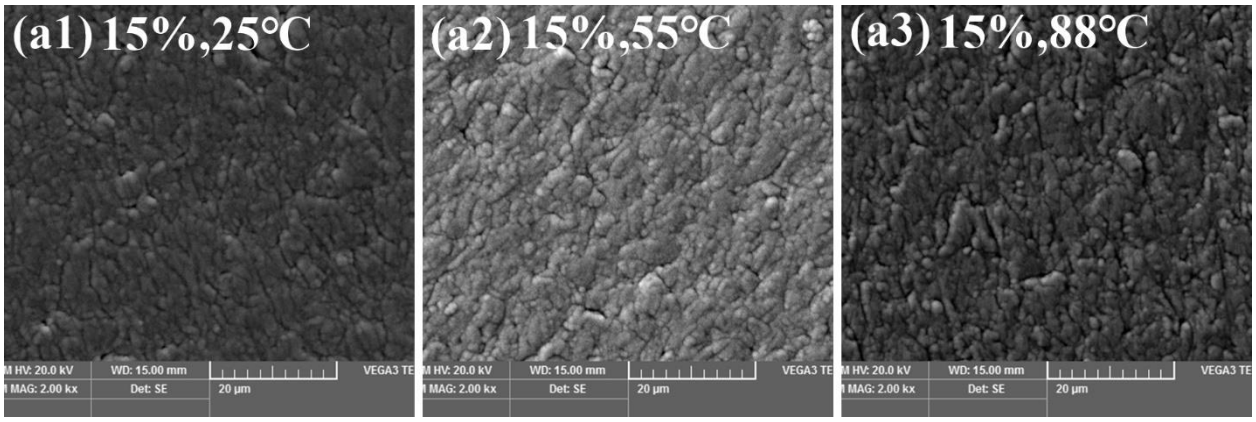

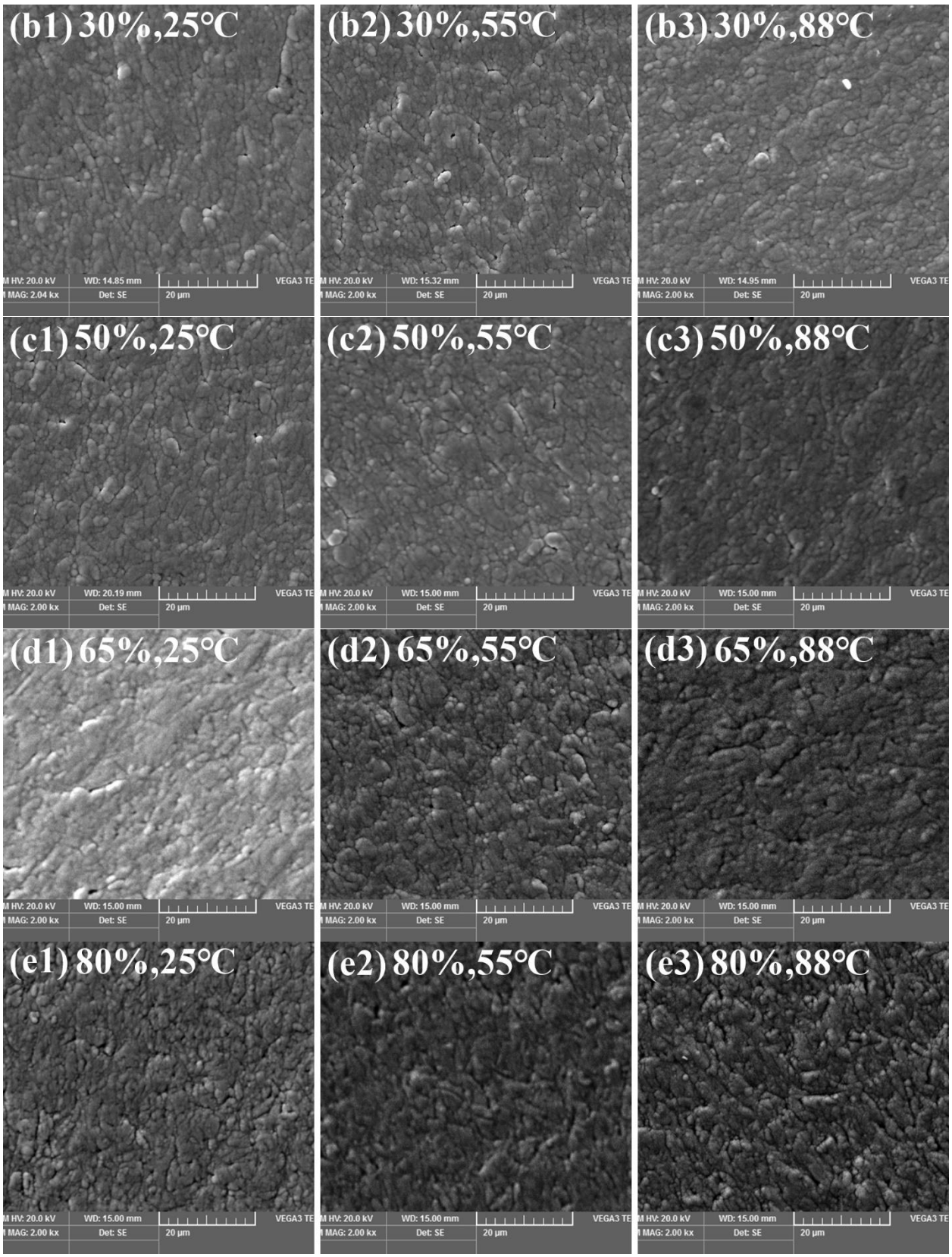

Figure 9. SEM micrographs of the ZrCrMoNb high-entropy alloy coating based on 3A21 aluminum alloy after electrochemical measurement in different concentrations of ethylene glycol solution at different temperatures.

Fig. 9 shows the scanning electron microscope test results of the ZrCrMoNb coating after the electrochemical test in the ethylene glycol solution. It can be clearly found that the corrosion becomes more obvious with the increase of temperature, and the corrosion of the ZrCrMoNb coating is also more serious at the same temperature when the ethylene glycol V/V concentration is 15% or 80%, they are consistent with the results of Potentiodynamic polarization and EIS.

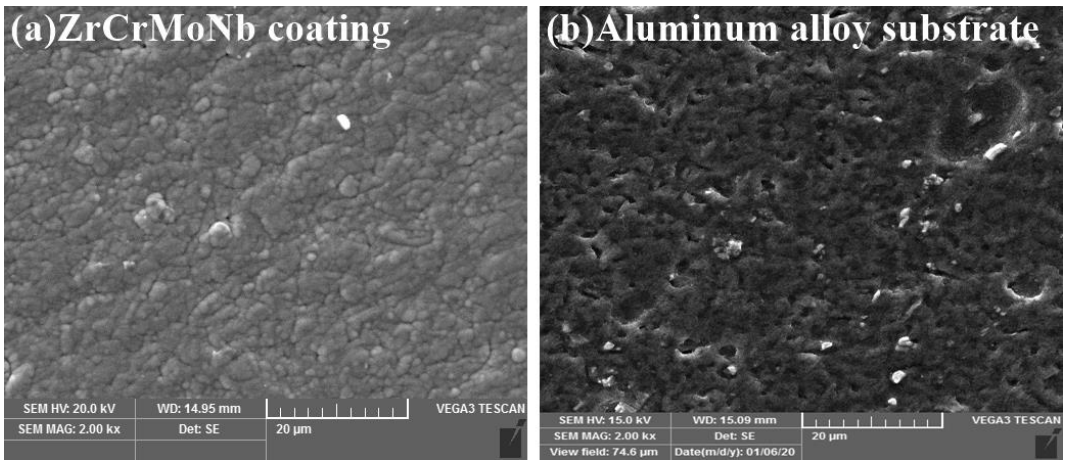

Figure 10. SEM micrographs of 3A21 aluminum alloy substrate at temperature of 88℃ after electrochemical measurement.

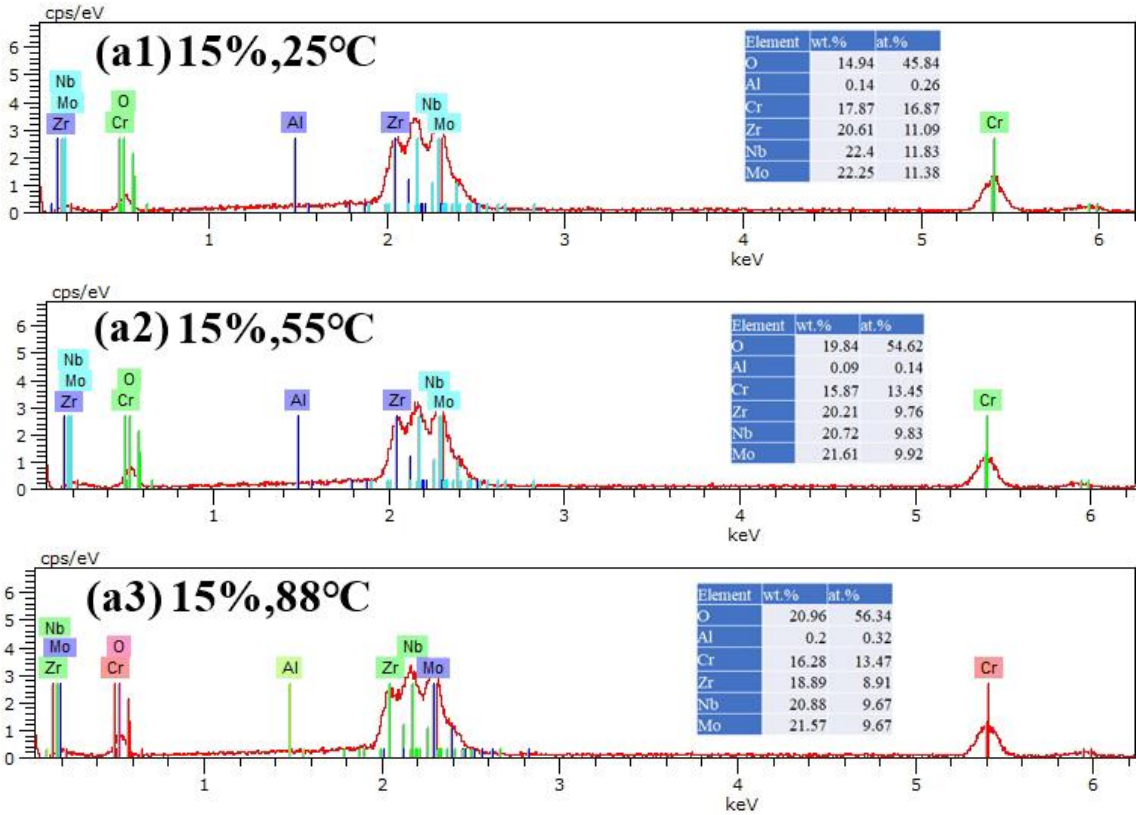

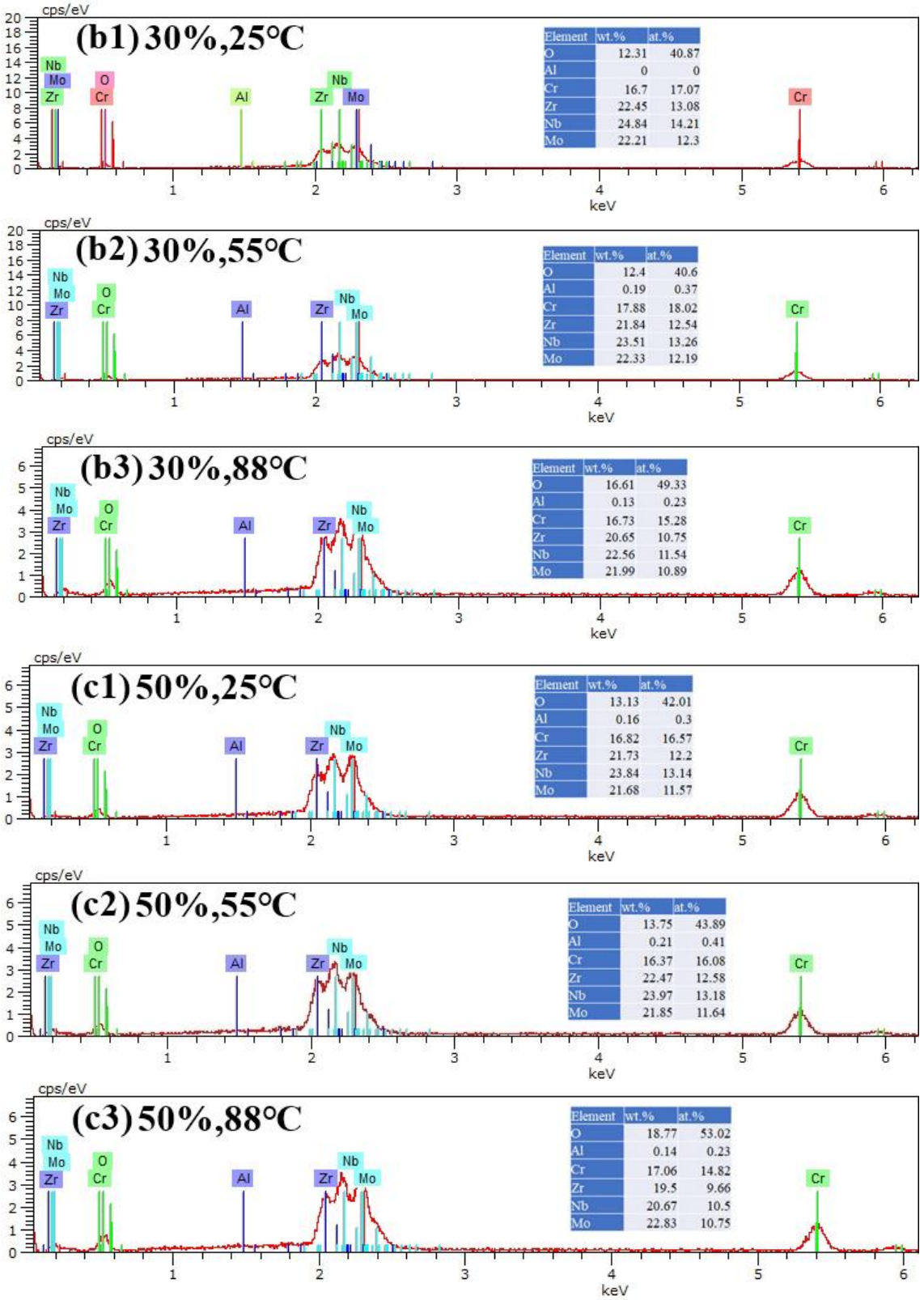
(b1) 30%,25°C
Element wt.% at.%
O 12.31 40.87
Al 0 0
Cr 16.7 17.07
Zr 22.45 13.08
Nb 24.84 14.21
Mo 22.21 12.3
(b2) 30%,55°C
Element wt.% at.%
O 12.4 40.6
Al 0.19 0.37
Cr 17.88 18.02
Zr 21.84 12.54
Nb 23.51 13.26
Mo 22.33 12.19
(b3) 30%,88°C
Element wt.% at.%
O 16.61 49.33
Al 0.13 0.23
Cr 16.73 15.28
Zr 20.65 10.75
Nb 22.56 11.54
Mo 21.99 10.89
(c1) 50%,25°C
Element wt.% at.%
O 13.13 42.01
Al 0.16 0.3
Cr 16.82 16.57
Zr 21.73 12.2
Nb 23.84 13.14
Mo 21.68 11.57
(c2) 50%,55°C
Element wt.% at.%
O 13.75 43.89
Al 0.21 0.41
Cr 16.37 16.08
Zr 22.47 12.58
Nb 23.97 13.18
Mo 21.85 11.64
(c3) 50%,88°C
Element wt.% at.%
O 18.77 53.02
Al 0.14 0.23
Cr 17.06 14.82
Zr 19.5 9.66
Nb 20.67 10.5
Mo 22.83 10.75
cps/eV
keV

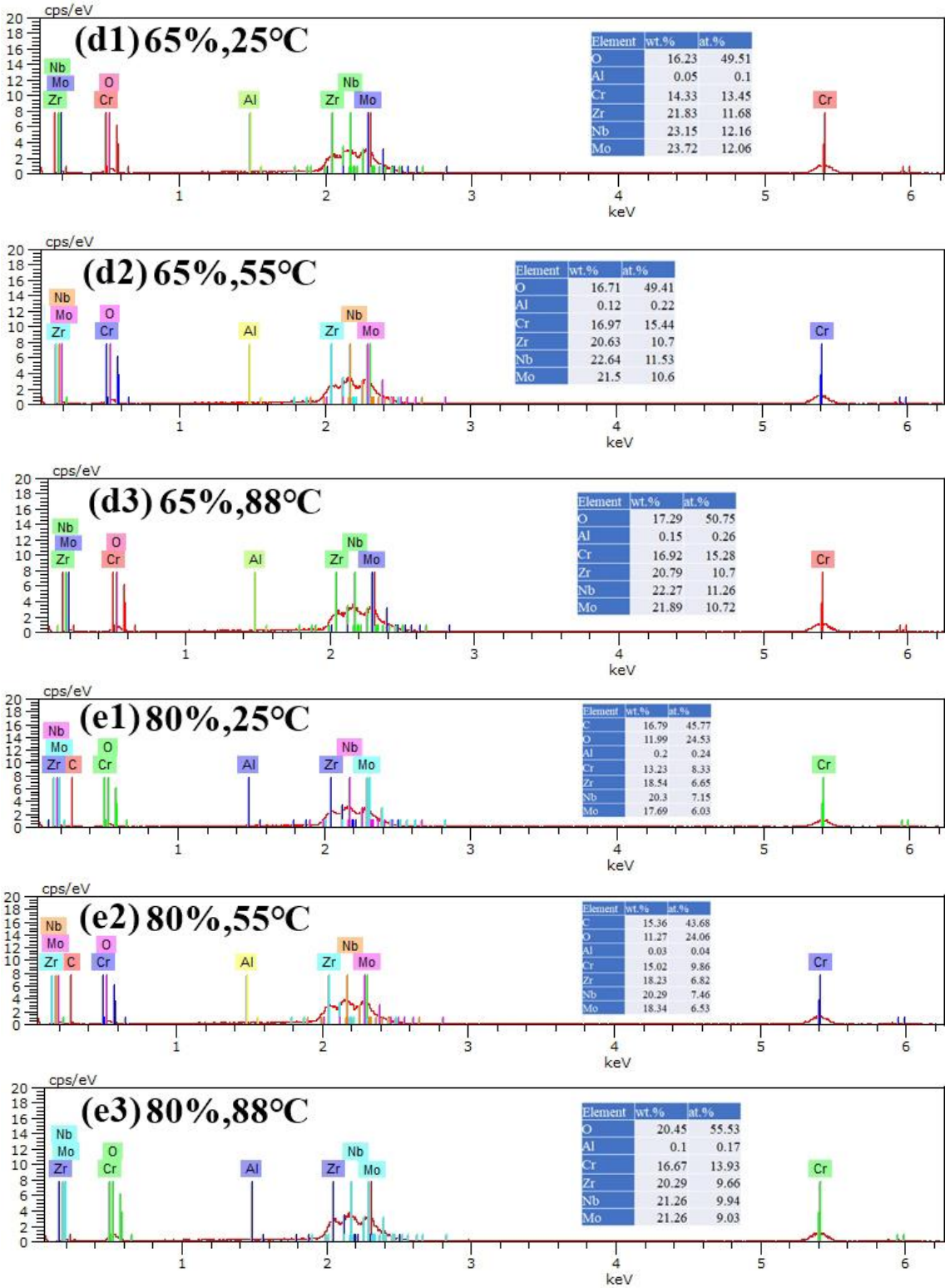

Figure 11. EDS micrographs of the ZrCrMoNb high-entropy alloy coating based on 3A21 aluminum alloy after electrochemical measurement in different concentrations of ethylene glycol solution at different temperatures.

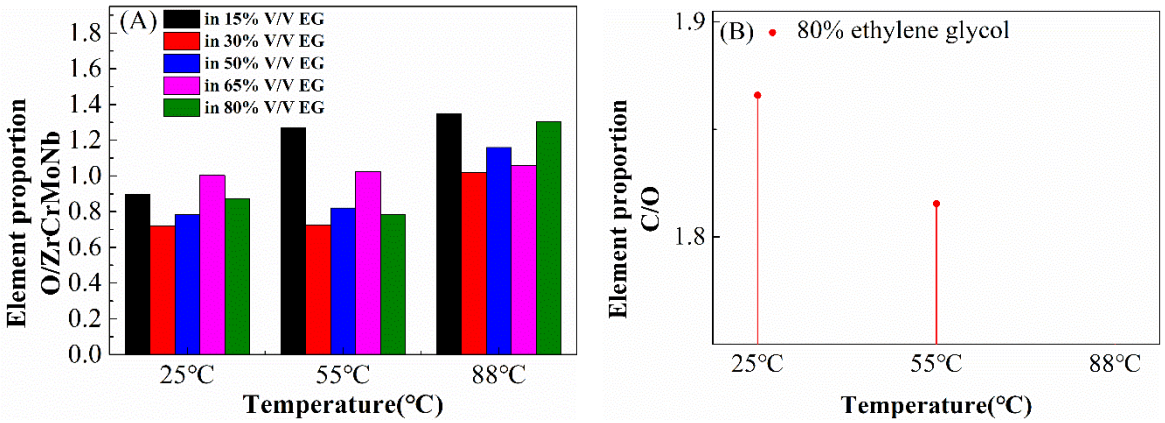

Figure 12. The element proportion on the surface of ZrCrMoNb coating in ethylene glycol solution.

Moreover, the experimental results also confirm that the ZrCrMoNb coating has better pitting corrosion resistance than the 3A21 aluminum alloy matrix in ethylene glycol solution, as shown in Fig. 10. Chen[27] found the corrosion of aluminum alloy was mainly pitting corrosion in ethylene glycol solution, it was Similar to the result in Fig. 10(b).

Fig. 11 shows the results of EDS of the ZrCrMoNb coating after the electrochemical test in the ethylene glycol solution. It is seen that the coating surface basically dose not contains aluminum element, indicating that 3A21 aluminum alloy substrate is not exposed to the ZrCrMoNb coating surface. All coating surfaces contain a certain amount of O element, suggesting that oxides were formed on the ZrCrMoNb coating surface. when the V/V concentration of ethylene glycol was 80%, C element was detected obviously on the surface of the ZrCrMoNb coating surface at the temperature is 25°C and 55°C. Moreover, it is also noted that the element ratio of O/ZrCrMoNb increases with the increase of temperature in the same V/V concentration of ethylene glycol solution, and in the 80% ethylene glycol solution, the element ratio of O/ZrCrMoNb reduced and that of C/O also significantly reduced when the temperature changed from 25°C to 55°C, which imply the formation of an alcohol film on the coating surface due to the adsorption of ethylene glycol[28] or its participation in the cathodic reaction, furthermore, the corrosion behavior of the coating was affected.

4. CONCLUSIONS

(1) The corrosion resistance of ZrCrMoNb high-entropy alloy coating would decrease with the increase of temperature in ethylene glycol solution. When the V/V concentration of ethylene glycol were 15% and 80%, the change of corrosion resistance with temperature was the most obviously.

(2) At the same temperature, the corrosion current density showed a significant decrease when the V/V concentration of ethylene glycol changed from 15% to 30%, and then the corrosion current density changed smoothly with increasing concentration. The 30% V/V concentration of ethylene glycol might be a critical point.

(3) The corrosion behavior of ZrCrMoNb high-entropy alloy coating in ethylene glycol is affected by the concentration of ethylene glycol and temperature, and the pitting corrosion resistance of the coating is better than that of aluminum alloy substrate.

ACKNOWLEDGEMENTS
This project is supported financially by the Program of Science & Technology Department of Sichuan Province (No. 2017JY0153), the Foundation of material corrosion and protection Key Laboratory of Sichuan Province (No. 2015CL05).

References

1. F.P. Incropera, *J. Heat. Trans-T. Asme.*, 110 (1988) 1097.
2. L. Niu and Y. Frank Cheng, *J. Appl. Electrochem.*, 42 (2007) 8613-8617.
3. D. Shen, G. Li, C. Guo, J. Zou, J. Cai, D. He, H. Ma and F. Liu, *Appl. Surf. Sci.*, 287 (2013) 451-456.
4. J.Zhao, L. Xia, A. Sehgal, D.Lu, R.L.McCreery and G.S.Frankel, *Surf. Coat. Technol.*, 140(1) (2001).
5. J.W. Yeh, S.K. Chen, S.J. Lin, J.Y. Gan, T.S. Chin, T.T. Shun, C.H. Tsau and S.Y. Chang, *Adv. Eng. Mater.*, 6(5) (2004) 299-303.
6. Tsai. M. H and Yeh J. W, *Mater. Res. Lett*, 2 (2014) 107-123.
7. H. Diao, L.J. Santodonato, Z. Tang, T. Egami and P.K. Liaw, *An Overview, Jom*., 67 (2015) 2321-2325.
8. Y.Y. Chen, U.T. Hong, J.W. Yeh and H.C. Shih, *Scr. Mater*., 54 (2006) 1997-2001.
9. M.H. Chuang, M.H. Tsai, W.R. Wang, S.J. Lin and J.W. Yeh, *Acta. Mater*., 59 (2011) 6308-6317.
10. C. Xiang, J.Z. Wang, H.M Fu, E.H. Han, H.F. Zhang, J.Q. Wang and Z.M. Zhang, *J. China. Soc. Corros. Prot.*, 36 (2016) 108-112.
11. Y.X. Liu, C.Q. Cheng, J.L. Shang, R. Wang, P. Li and J. Zhao, *Trans. Nonferrous Met. Soc. China.*, 25 (2015) 1341-1351.
12. K.Y. Tsai, M.H. Tsai and J.W. Yeh, *Acta Mater*., 61 (2013) 4887-4897.
13. W. Zhang, M. Wang, L. Wang, C.H. Liu, H. Chang, J.J. Yang, J.L. Liao, Y.Y. Yang and N. Liu, *Appl. Surf. Sci*., 485 (2019) 108-118.
14. W. Zhang, R. Tang, Z.B. Yang, C.H. Liu, H. Chang, J.J. Yang, J.L. Liao, Y.Y. Yang and N. Liu, S*urf. Coat. Technol*., 347 (2018) 13-19.
15. W. Zhang, R. Tang, Z.B. Yang, C.H. Liu, H. Chang, J.J. Yang, J.L. Liao, Y.Y. Yang and N. Liu, *J. Nucl. Mater*., 512 (2018) 15-24.
16. A. D1384-01, *Annual Book of ASTM standards*., (2005).
17. H.S. Medhashree and Adka Nityananda, *J. Adhes. Sci. Technol*., 33 (2018) 523-548.
18. A. Conde and J.D. Damborenea, *Corros. Sci.*, 39(1) (1997) 295-303.
19. F.J. Martin, G.T. Cheek, W.E. O'Grady and P.M. Natishan, *Corros. Sci.*, 47 (2005) 3187-3201.
20. C. Liu, M. Gong and X.W. Zheng, *Int. J. Electrochem. Sci*., (2018) 7432-7441.
21. P.B. Su, X.H. Wu, Y. Guo and Z.H. Jiang, *J. Alloys Compd*., 475 (2009) 773-777.
22. P. Zoltowski, *J. Electroanal. Chem*., 443(1) (1998) 149-154.
23. R.X. Qiu, Z.X. Li and Z.L. Wu, *Mater. Res. Express*., 6 (2019) 045059
24. Y. Shi, C. Ni, J. Liu and G.Z. Huang, *Mater. Sci. Technol*., 34 (2018) 1239-1245.
25. X. Li, P.L. Mao, F. Wang, Z. Wang, Z. Liu and L. Zhou, *Mater. Res. Express*., 5 (2018)106507
26. T.S. Hua, R.G. Song, Y. Zong, S.W. Cai and C. Wang, *Mater. Res. Express*., 6 (2019) 096441
27. X. Chen, W.M. Tian, S.M. Li, M. Yu and J.H. Liu, *Chin. J. Aeronaut.*, 29 (2016) 1142-1150.
28. H.Y. Zuo, M. Gong, X.W. Zheng, L. Wang and W. Emori, *Mater. Res. Express*., 7 (2020) 026523